International Journal of Computer Information Systems and Industrial Management Applications.
ISSN 2150-7988 Volume 10 (2018) pp. 183–196

Improving Reduced Reference Image Quality Assessment Methods By Using Color Information

Mounir Omari[1],Abdelkaher Ait Abdelouahed[2], Mohammed El Hassouni[1] and Hocine Cherifi[3]

[1] Faculty of Science, LRIT Associated Unit to the CNRST, URAC 29, Mohammed V University, Rabat, Morocco.
mouniro870@gmail.com, mohamed.Elhassouni@gmail.com

[2] LABSIV (laboratoire des systémes informatiques et vision) - IBN ZOHR University, Agadir, Morocco.
a.abdelkaher@gmail.com

[3]LE2I UMR 6306 CNRS, University of Burgundy, Dijon, France.
hocine.cherifi@u-bourgogne.fr

Abstract: **In real-world applications, images and videos are often acquired and displayed in color. To assess the quality of these images, most of the methods have been developed in a grayscale level without considering the color information. Among the methods that remain less explored in color, one can find reduced reference image quality assessment (RRIQA) methods and especially those based on natural scenes statistics (NSS). Motivated by the close relationship that lies between inter/intra-color components perception and statistics, this paper proposes a new framework to study the impact of color information on RRIQA methods and more specifically the NSS based ones. For this purpose, the inquiry investigates how each information (luminance, chrominance) influences the quality assessment process. Then, it also considers whether the combination of these components can improve the quality prediction scores. The deployment of this framework is closely related to the choice of quality methods and perceptual color spaces. Thus, four of the most influential RRIQA based NSS methods have been intuitively extended to color. Furthermore, YCbCr and CIELAB color spaces are selected thanks to their usefulness to separate chrominance and luminance information. On an experimental level, these methods are implemented on TID2013 benchmark, which offers a wide range of color specified distortion types. The obtained results showcase how color information can improve quality scores.**

Keywords: Reduced reference measure, natural image statistics, image quality assessment, color spaces

I. Introduction

In the last years, the research carried out by various laboratories in image quality assessment have conducted their metrics on grayscales level [1–3]. However, the human visual system perceives images in color. Therefore, this paper intends to show the need for all information in color image quality assessment, including color information.

In this area, one can distinguish three categories of measures: full reference (FR) [4] measures compare the distorted image with its reference version. These measures are believed to be the most accurate and robust, but, the reference image is not always available in all practical situations. No reference (NR) [5–11] measures are computed directly from the degraded image. These measures often require, but not always, a prior knowledge about the distortion in the image to be evaluated. Whereas RR measures, need only a description about the reference image, and generally no a prior knowledge. Thus, they are more suited to a specific situation. Reduced-reference (RR) measures compare a description of the distorted image and the same description of the reference version, where a description is a set of relevant features extracted from both images. The performance of quality measure and its general-purpose depend on the amount of the available information. Therefore, they can be designed for general-purpose. The implementation of these measures can involve images distortion modeling [12, 13], human visual system modeling [14, 15] or natural scene statistics (NSS) modeling [16, 17].

Most of these measures were designed primarily to assess the quality of the image on the grayscale level, while the human eye perceives the world scenes in color. In literature, there are few RRIQA methods that have developed appropriate metrics for color images [18–20], and especially those based on NSS. Decherchi et al. [21] use two-layer architecture in order to predict the quality score. The first layer identifies the distortion, the second layer predicts the visual quality according to this specific distortion. Both luminance and chrominance information are applied for extracting descriptors to feed the predictor. Despite its good performance, this method has an inconvenient of the features vector size. Another work from Redi et al. [22] uses descriptors from HSV and YCbCr color spaces. The hue and the luminance channels are used in the HSV and YCbCr color spaces, respec-

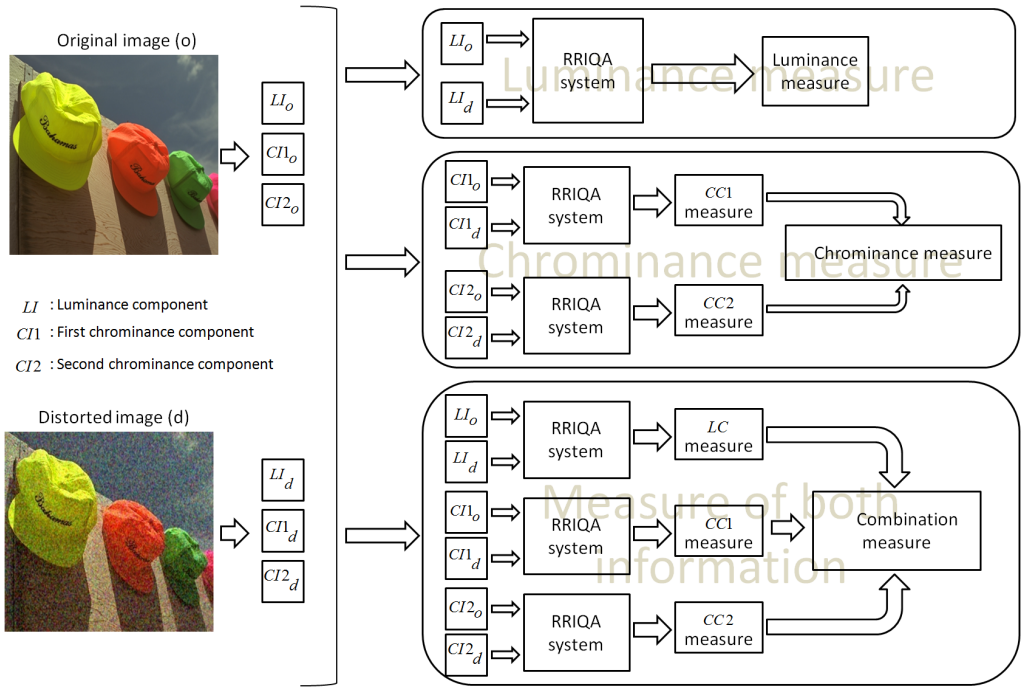

Figure. 1: The deployment of the proposed framework using three sorts of measures.

tively. A computational intelligence paradigm is also applied with two layers. As the method of Decherchi et al., the first layer is based on neural classification to identify the kind of distortion while the second layer quantifies the quality prediction using neural regression machine. This approach has the same weakness as Decherchi's one.

There is another color based RRIQA method developed by He et al. [23]. The extracted features using a color fractal structure model, are mapped to visual quality using the support vector regression. Their method demonstrates good performances on the LIVE Benchmark, but, it has only implemented on RGB color space and so the perceptual aspect has not been taken into account. Despite there appropriateness to color images, these RRIQA methods do not take in consideration statistical properties of color components which present a perceptually relevant tool for real-world images quality. In a preliminary work [24], the introducing of the color information into RRIQA process increases the quality scores in certain cases compared to grayscale level.

Recently, Ghadiyaram *et al.* [25] conducted an investigation to determinate how the chrominance information can improve the blind image quality prediction. According to their results, they offered a model called FRIQUEE (Feature maps based Referenceless Image Quality Evaluation Engine) to consolidate the process of the prediction with the chrominance information. Nonetheless, they are interested only in LIVE benchmark, which lacks a wide range of color specified distortions. In addition, despite its relevance, this method is NR which is out of the scope of our study. In this way, this paper aims to find how chrominance, luminance or the combination of both of them can enhance the RRIQA process. To respond to this question, and since all NSS reduced reference color image quality assessment processes [26–31] do not benefit from color information four of the most relevant natural scenes statistics RRIQA methods are employed. As these methods have been implemented in grayscale level, the first step consists of using their extension to color. For this extension, two color spaces (CIELAB, YCbCr) are investigated. The choice of these spaces depends especially on the separation of the three channels into two categories (Chrominance channels, and luminance channel).

A fair comparison between these categories using the four aforementioned methods has been done on the TID2013 benchmark.

This paper is organized as follows. Section II presents the selected methods and the proposed framework to compare the luminance channel, the chrominance channels, and the combination between both of them, and explains the characteristics of the two chosen color spaces. Section III concerns the experimental data and the validation protocol. Section IV details the experimental results and finally concluding remarks are presented in Section V.

II. Using color for RRIQA based NSS methods

In light of the worldwide, the human eye can not separate the chrominance from luminance, indeed, the human eye sees the world in color. Thus, one cannot exclude either the chrominance information (CI) nor the luminance information (LI). Recently, most commonly known RRIQA methods [4–8] have addressed the image in grayscale level, which presents a huge drawback in term of reliability. To emphasize this issue, Omari *et al.* [24] accentuates the effectiveness of CI in image prediction domain, four of the well-known methods have been handled in a manner more intuitive to itemize the usefulness of chrominance. This paper has proved without a doubt that these methods are poorly arranged with CI, which leads us to bring a solution to remedy this problem.

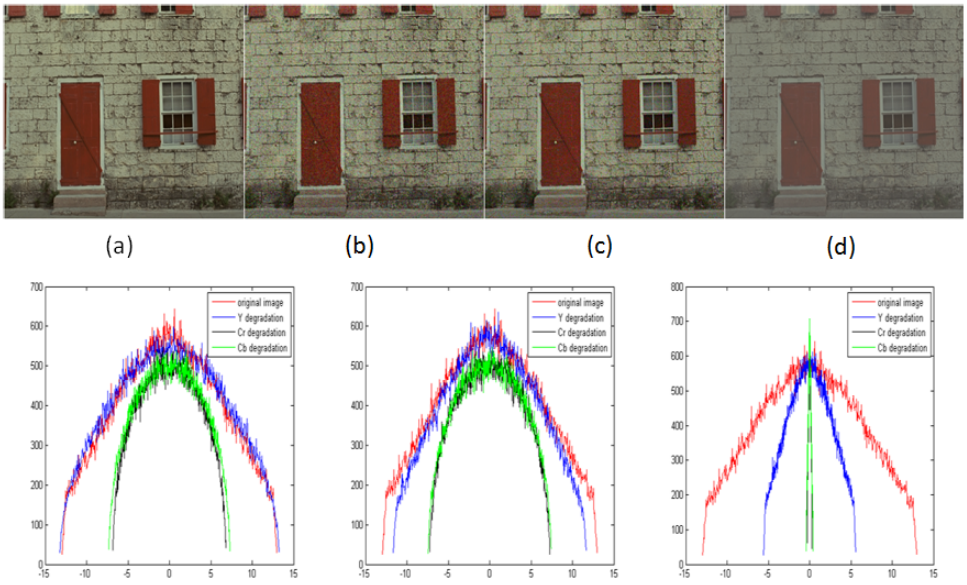

Figure. 2: Histogram of normalized coefficients: the first row depicts the images, from left to right: (a) the original image, (b), (c), and (d) are an image (a) distorted with Additive Gaussian noise, Additive noise in color components, and Contrast change respectively. The second row gives a statistical comparison between the original image (a) and the three distorted images: Red curve presents the original image, where, Blue, Black and Green curves are Y, Cr and Cb components of a distorted image, respectively.

A. Proposed framework

To reply to the previous ubiquitous question, and according to the results of [24], such distortions are convenient with CI where others are appropriate with LI. Therefore, this framework develops three types of measures, one addresses the luminance information, where the remaining two measures intended to add the chrominance information onto the debate. For greater certainty, Figure 1 depicts the track from original and distorted images to the three measures. So, the first step is related to the extraction of the three components. The second step is dedicated to computing quality using the following measures:

- The first measure considers the luminance components with a simple way to prescribe the luminance measure.
- The second measure retakes the chrominance components to adjust the chrominance measure, the two metrics between the four chrominance components are added up in order to reach the extent desirable.
- Finally, the third measure is the sum of the chrominance and the luminance measures.

B. Perceptual color spaces and statistical dependence

As mentioned above, the inquiry role is to investigate the color spaces which separate CI from LI. Thus depending on the circumstances of the current subject, the RGB color space is unlikely to be linked to the present study. This claim leads us to redirect this paper into the perceptual color spaces. Humans can perceive thousands of colors, and only about a couple of dozen gray shades. Based on this assumption, two color spaces are proposed (CIELAB and YCbCr).

The CIELAB [32] color space contains all perceivable colors, which means that the gamut of CIELAB exceeds the gamut of the RGB color space, where L stands for lightness and a and b for the color-opponent dimensions. Usually, the fact that the CIELAB [33–35] is described as a color appearance model gives a negative reaction to the the most of colorimetry peoples. It is considered as a device-independent. Hence, it is impossible to produce the range of luminance and chromatic contrast that is witnessed in the original scene. However, the CIEXYZ is proposed to get an approximation of the three components.

The demands for digital algorithms in handling video information have found a solution with the YCbCr [22] color space and have become a widely used model in a digital video. Y is the luminance component which computed from nonlinear RGB [36] by using a weighted sum of RGB values. Cb is the difference between blue and luminance components and Cr is the difference between red and luminance components [37, 38].

To represent the color information in a statistical manner, Figure 2 compares the behavior of different color distributions and the grayscale. In the second row at the far left, four histograms have been remarked, the red one represents the normalized coefficients of the original image in grayscales level, the three others represent the histograms of the three components of YCbCr of image 2(b), the chrominance histograms (green and black) are clearly far from the histogram of the original image which is not the case for the luminance histogram (blue). The graphics on the middle and on the right prove the chrominance adequacy to represent Additive noise in color components and Contrast change respectively. However, the intuitive extension proposed in this paper brought together the two chrominance components. Thus, to illustrate the statistical dependency of intra-component for luminance and inter-components for chrominance, Chi-plot graphs [39] are used to observe the different types of depen-

dency. This latter can be considered as an extension of the scatterplot which is usually employed to illustrate a possible dependency. A common setting has been used as it is noted in [39] to define the tolerance band which is shown as a gray-shaded region. A deviation from the tolerance band indicates a dependence structure. Figure 3 shows a set of Chi-plots for CIELAB and YCbCr. The steerable pyramid transform [40] enables to get the chi-plots. First of all, for the luminance channel for both CIELAB and YCbCr, two subbands have been selected from the same level to see the inter-orientation dependency. For the chrominance part, the two channels are used to get the chi-plot between them. As concerns the luminance components (first column), the chi-plots show the high inter-orientation dependency found between adjacent sub-bands for a same scale decomposition level for the luminance channel. For the chrominance channels (second column), the dependency between the two channels is clearly seen with a negative chi χ for YCbCr and a positive chi χ for CIELAB.

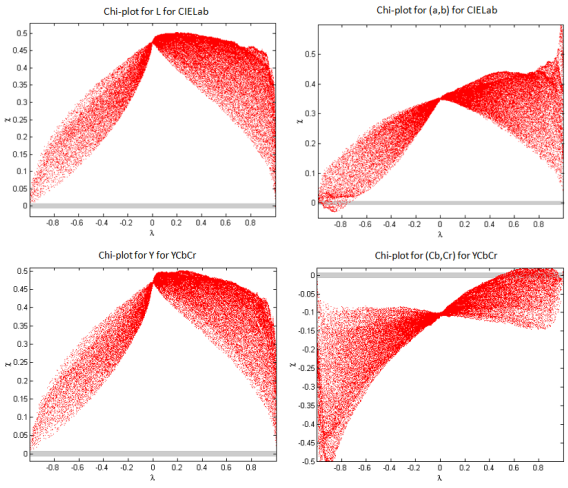

Figure. 3: Chi-plots to show the statistical dependency of intra-component for luminance and inter-components for chrominance.

C. Studied RRIQA based NSS methods

The Reduced Reference methods for image quality assessment in grayscale levels have known a glut, starting by modeling image distortions and modeling the human visual system and going to modeling natural image statistics. Nevertheless, these processes may be reconsidered in the future if and when the grayscale levels evolve to multi-color channels. Therefore, four of the most commonly cited methods have been selected.

1) WNISM [16](Wavelet-Domain Natural Image Statistic Model)

The transform used for this method is the steerable pyramid [40] in order to decompose an image into scale and orientation subbands in an efficient and accurate manner. The generalized Gaussian density (GGD) is the distribution used for subbands modeling. The statistical framework to estimate and compute efficiently the parameters of GGD is the Maximum Likelihood. Afterward, the overall distortion measure is the sum of the Kullback-Leibler Divergence (KLD) of all subbands. It should be noted that there exists a closed-form expression for the KLD to quantify the difference between the model parameters of the GGD.

2) DNT [41](Divisive Normalization Transform)

Statistical and perceptual issues Motivated Li *et al.* [41] to substitute the steerable pyramid representation by a divisive normalization transform (DNT). They propose a two-stage procedure, a wavelet image decomposition, followed by a divisive normalization stage. First of all, an initial model based on the Gaussian Scale Mixture (GSM) for the wavelet coefficients [42] is called. It is a result of the product of two independent components; a zero-mean Gaussian random vector with covariance and a scalar random variable called a mixing multiplier. As well as WNISM, the DNT computed coefficients are based on the maximum-likelihood estimate of the multiplier. Finally, the quality score is then computed using the KLD between the zero-mean Gaussian models.

3) EMISM [17](Empirical Mode Image Statistic Measure)

In [17], authors choose the bidimensional empirical mode decomposition (BEMD) as a transformation domain. This procedure is based on the frequency-time analysis, each image is decomposed into a number of intrinsic mode functions (IMFs) and a residue. To model the visual information in a suitable manner, an adaptive analysis is allowed from the basic functions of the EMD derived from the image content.

Indeed, the main drawback of the steerable pyramid representation is that the basis functions are fixed and do not necessarily match the varying nature of images. Experimental results have shown that the GGD is a good fit for the IMF distribution. The distortion measure is computed based on the KLD between the IMF statistics.

4) RRED [43](Reduced Reference Entropic Differencing)

The Soundararajan et al. [43] propose a measure based on entropy. The principal idea is to link the distortion to the entropy difference between the wavelet coefficients. First step based on splitting a selected sub-band into blocks, and then computing the entropy of each block, assuming a GSM model. Then, they calculated the difference between the entropies of the original and degraded blocks in order to find the overall distance. There is two way to compute the overall measure, the first one is the summation of the entropies difference, the second one is the difference between the summation of the entropies of the blocks.

III. Experimental setup

A. Dataset

The TID2013 dataset [44,45] is used to test the performances of the measures under investigation. This recently released benchmark is an improved version of the TID2008 database. It has the same number of reference images as TID2008, with 3000 distorted images (25 reference images with 24 types of distortions and 5 levels of distortions). The quality of each image in TID2013 has been graded by the Mean Opinion

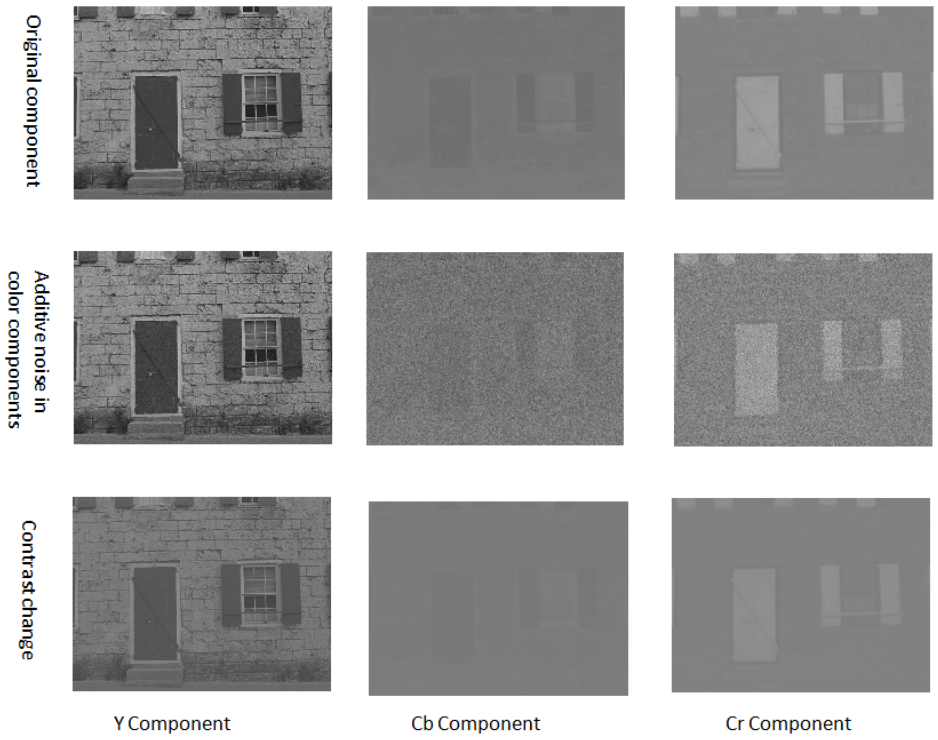

Figure. 4: Two artifacts from two different kinds of distortions influencing the three components of YCbCr.

Method	EMISM [17]	WNISM [16]	DNT [41]	RRED [43]
Information	Luminance			
Number of features	12	18	48	$L/36$
Information	Chrominance			
Number of features	24	36	96	$(2 \times L)/36$
Information	Luminance+Chrominance			
Number of features	36	54	144	$(3 \times L)/36$

Table 3: The numbers of features for the four selected methods (L is the size of the image).

Score (MOS) and experiments was carried out by 971 observers.

In scrutinizing TID2013, according to Ponomarenko et al. in [46], only three chrominance distortions (Additive noise in color components, Quantization noise, JPEG compression) have been token in TID2008. Owing to the lack of chrominance distortions, Ponomarenko et al. [44] have developed TID2008 into TID2013 to append new distortion types, especially the chrominance distortions. For the purpose of the current study, the distortion types of TID2013 can be divided into two categories: Color distortions and Luminance distortions. The first category has been prescribed in Table III-A. For the luminance distortions, one can find eighteen distortion types mentioned in Table III-A. The wealth of the chrominance distortions for this newest benchmark strongly motivates our choice, to parse the impact of chrominance, luminance, and combination on each category.

In Figure 4, the three components of YCbCr color space altered by two distortions: the additive noise in color components that belongs to chrominance distortions; and the contrast change that belongs to luminance distortions, show that the influence of the first artifact is clearly remarked for Cb and Cr components, on the contrary for the Y component. As regards the second artifact, it affected the Y component more than the Cb and the Cr components.

Label	Type of distortion
1	Additive noise in color components
2	Quantization noise
3	JPEG compression
4	Change of color saturation
5	Image color quantization with dither
6	Chromatic aberrations

Table 1: The six chrominance distortion types in TID2013.

Label	Type of distortion
1	Additive Gaussian noise
2	Spatially correlated noise
3	Masked noise
4	High frequency noise
5	Impulse noise
6	Gaussian blur
7	Image denoising
8	JPEG2000 compression
9	JPEG transmission errors
10	JPEG2000 transmission errors
11	Non eccentricity pattern noise
12	Local block-wise distortion of different intensity
13	Mean shift
14	Contrast change
15	Multiplicative Gaussian noise
16	Comfort noise
17	Lossy compression of noisy images
18	Sparse sampling and reconstruction

Table 2: The eighteen luminance distortion types in TID2013.

B. Experimental protocol

1) Validation protocol

To compare the proposed measure with the subjective quality score (MOS), a nonlinear regression using a logistic function in order to map the objective and subjective scores [47] is performed. To do so, a logistic function is proposed by the Video Quality Expert Group (VQEG) Phase I FR-TV with five parameters. The expression of the quality with five parameters. The expression of the quality score which is the predicted MOS is given by:

$$DMOS_p = \beta_1 \text{logistic}\left(\beta_2, D - \beta_3\right) + \beta_4 D + \beta_5. \quad (1)$$

Where the vector $(\beta_1, \beta_2, \beta_3, \beta_4, \beta_5)$ is estimated thanks to *fminsearch* function in the optimization Toolbox of Matlab, and the logistic function is expressed by :

$$\text{logistic}\left(\tau, D\right) = \frac{1}{2} - \frac{1}{1 + \exp\left(\tau D\right)}. \quad (2)$$

Where D is the distortion measure in Figure 1.

The prediction accuracy is measured by the Pearson's linear correlation coefficient PLCC to evaluate the relevance of a quality metric. This coefficient is defined as follows:

$$PLCC = \frac{\sum_{i=1}^{n}(s_i - \bar{s})(x_i - \bar{x})}{\sqrt{\sum_{i=1}^{n}(s_i - \bar{s})}\sqrt{\sum_{i=1}^{n}(x_i - \bar{x})}}, \quad (3)$$

Where s_i is the subjective score of the i^{th} image, x_i represents the predicted MOS defined in equation 1 of the i^{th} image, and $(\bar{s}, \bar{x})$ denote respectively the average of (s, x).

2) Adaptation protocol for color information categorization

In the present study, a new framework to integrate color information into RRIQA procedures is proposed. However, the term "reduced reference" must be taken into account, while keeping a good correlation with MOS scores. In this sense, Table III-A shows a comparison between the number of features required by each color information for the studied quality methods. the results demonstrate that LI remains the least expensive information in terms of features number followed by the chrominance information CI, and the last is the combination of both LI and CI. Until now, the features size of each color information was not incorporated in the proposed framework prescribed in subsection II-A.

As the main objective of this study is to find what quality color information-based measure is more appropriate for which type of distortion, a protocol of information adaptation is enclosed to the current framework. Figure 5 illustrates the mechanism of the adaptation protocol. Firstly, the three measures in Figure 1 have been used for the development of the proposed framework. The idea behind the adaptation protocol is undoubtedly related to the choice of the information. Therefore, in order to apply the adaptation protocol, the following equation is employed:

$$\Delta\left(x, y\right) = \left(\left(x - y\right)/y\right) * 100 \quad (4)$$

Where $\Delta\left(x, y\right)$ represents the percentage of variation between two values (x, y).

Label	EMISM [17]						WNISM [16]					
	CIELAB			YCbCr			CIELAB			YCbCr		
	Chrominance distortions											
	L	AB	Lab	Y	CbCr	YCbCr	L	AB	Lab	Y	CbCr	YCbCr
1	0.51	**0.73**	0.63	0.44	0.60	0.60	0.70	**0.86**	0.80	0.65	**0.86**	0.78
2	0.73	0.79	0.79	0.66	**0.74**	0.73	**0.72**	0.66	0.70	0.62	**0.68**	0.65
3	0.81	**0.88**	0.70	0.68	**0.75**	0.69	0.78	0.67	**0.81**	0.87	0.81	**0.90**
4	0.24	**0.68**	0.25	0.27	**0.62**	0.25	0.11	0.65	**0.67**	0.22	0.51	**0.58**
5	0.65	0.46	**0.78**	0.64	0.44	**0.72**	**0.75**	0.56	0.73	**0.52**	0.29	0.51
6	0.83	0.52	**0.94**	0.45	0.45	**0.82**	**0.93**	0.32	0.80	**0.96**	0.19	0.78
	Luminance distortions											
1	0.66	**0.79**	0.71	0.56	**0.74**	0.68	0.80	**0.90**	0.87	0.71	**0.92**	0.78
2	0.70	**0.79**	0.68	0.58	**0.74**	0.61	0.81	**0.89**	0.87	0.71	**0.91**	0.82
3	0.53	**0.66**	0.62	0.43	**0.67**	0.63	0.66	0.70	**0.74**	0.66	0.65	**0.72**
4	0.78	**0.85**	0.79	0.70	**0.83**	0.73	0.88	**0.95**	0.92	0.79	**0.94**	0.91
5	0.44	0.49	**0.54**	0.39	0.31	**0.46**	0.73	0.79	**0.81**	0.67	0.77	**0.80**
6	0.78	0.79	**0.89**	0.77	0.87	**0.94**	**0.94**	0.81	0.90	**0.91**	0.50	0.83
7	0.54	0.61	**0.81**	0.39	0.60	**0.78**	**0.93**	0.46	0.83	**0.88**	0.38	0.82
8	0.67	0.81	**0.89**	0.62	0.76	**0.80**	**0.95**	0.78	0.89	**0.93**	0.56	0.87
9	**0.64**	0.61	0.46	**0.64**	0.09	0.34	**0.81**	0.45	0.68	**0.88**	0.11	0.67
10	**0.68**	0.67	0.60	**0.63**	0.33	0.54	**0.84**	0.61	0.74	**0.79**	0.09	0.72
11	0.25	0.25	**0.56**	0.20	0.24	**0.46**	0.39	0.34	**0.46**	**0.42**	0.04	0.34
12	0.08	0.03	**0.29**	0.19	0.25	**0.39**	0.22	0.08	**0.25**	0.21	0.04	**0.23**
13	0.75	0.75	0.58	0.18	**0.46**	0.43	0.72	0.68	**0.73**	0.47	0.11	**0.52**
14	**0.60**	0.35	0.45	0.59	**0.62**	0.53	**0.57**	0.26	0.38	**0.72**	0.20	0.54
15	0.57	**0.71**	0.68	0.54	0.60	**0.61**	0.82	**0.86**	0.85	0.63	**0.81**	0.79
16	0.38	**0.63**	0.45	0.05	0.07	**0.21**	0.53	0.48	**0.56**	0.71	0.11	**0.73**
17	**0.68**	0.67	0.67	0.65	**0.73**	0.71	0.80	0.82	**0.91**	0.76	0.78	**0.92**
18	**0.94**	0.87	0.91	**0.89**	0.44	0.88	**0.93**	0.78	0.89	**0.91**	0.39	0.86

Table 4: The Pearson's linear correlation coefficients (PLCC) for EMISM and WNISM in TID2013 benchmark.

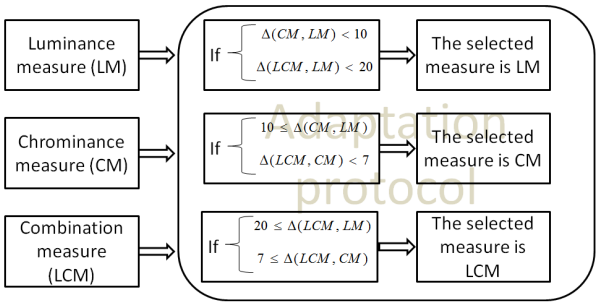

Figure. 5: The description of the proposed protocol of adaptation using the three quality information-based measures LM, CM and LCM presented in Figure 1.

According to the features sizes in Table III-A, three thresholds (10% between LI and CI, 20% between LI and the combination (LCM), and 7% between CI and the combination) have been accorded for the adaptation protocol.

IV. Experimental results

The previous section looked at the selected benchmark and experimental protocol. In real-world, the most perceptual information is the chrominance, therefore, this section searches for the importance of this information in well-known RRIQA methods. Thus, for the purpose of the current study, this section is organized as follow. First of all, a simple comparison between the chrominance and the luminance impact despite the features size has been made. Afterward, the combination of both information can also improve the performances. Therefore, this framework compares the best scores between LI and CI against the combination scores to seek for the better of choices. Finally, the adaptation protocol is established in order to retrieve the convenient information for each distortion type.

A. *Comparison between chrominance and luminance impact for each method*

Table III-B.2 reports the prediction accuracy for both methods EMISM and WNISM, in both color spaces CIELAB and YCbCr. In order to compare the impact of the luminance and the chrominance for each method, the table provides results for both types of distortions in TID2013 database: luminance distortions and chrominance distortions. Let us start with the EMISM method, for chrominance distortions and as expected, the chrominance gives the best quality scores for four distortion types (1, 2, 3, and 4) for both color spaces. In the same Table for the two others chrominance distortions, suddenly, the domination has been swapped between chrominance and luminance.

Label	DNT [41]						RRED [43]					
	CIELAB			YCbCr			CIELAB			YCbCr		
	L	AB	Lab	Y	CbCr	YCbCr	L	AB	Lab	Y	CbCr	YCbCr
	Chrominance distortions											
1	0.38	0.67	0.67	0.26	**0.54**	0.53	0.80	0.85	0.85	0.79	0.84	**0.86**
2	0.34	0.67	**0.68**	0.24	0.63	**0.65**	**0.77**	0.73	0.76	0.77	**0.81**	0.80
3	**0.78**	0.75	0.77	0.55	0.46	0.55	**0.94**	0.80	0.89	**0.94**	0.88	0.91
4	0.08	0.48	0.48	0.25	0.44	**0.46**	0.63	0.65	0.65	0.22	**0.70**	0.69
5	**0.72**	0.57	0.57	0.33	**0.45**	0.43	**0.85**	0.78	0.84	0.60	0.58	**0.61**
6	**0.90**	0.30	0.75	**0.91**	0.21	0.77	**0.94**	0.71	0.90	**0.95**	0.62	0.92
	Luminance distortions											
1	0.69	0.78	0.78	0.60	0.62	0.62	0.79	0.87	0.87	0.80	0.91	0.91
2	0.41	0.69	0.69	0.32	**0.64**	0.63	0.78	**0.87**	0.86	0.79	**0.91**	0.89
3	0.46	0.59	0.59	0.22	0.66	**0.67**	0.47	**0.61**	0.59	**0.84**	0.77	0.81
4	0.52	0.80	0.80	0.41	**0.76**	0.75	0.88	0.94	0.94	0.86	**0.95**	0.94
5	0.51	0.52	0.52	0.45	0.54	**0.55**	0.77	0.85	**0.86**	0.78	0.85	**0.87**
6	0.85	0.85	0.82	0.82	**0.85**	0.83	0.90	0.86	**0.94**	0.91	0.87	**0.93**
7	**0.88**	0.64	0.86	**0.87**	0.68	0.85	**0.94**	0.83	0.91	**0.94**	0.86	0.93
8	**0.94**	0.88	0.90	**0.90**	0.82	0.88	**0.94**	0.70	0.90	**0.97**	0.74	0.92
9	**0.75**	0.45	0.49	**0.32**	0.20	0.28	**0.89**	0.62	0.80	**0.89**	0.48	0.77
10	0.45	0.15	**0.58**	0.75	0.07	**0.82**	0.74	**0.77**	0.70	0.76	**0.81**	0.73
11	0.28	0.31	**0.40**	0.18	0.28	**0.34**	0.77	0.80	**0.82**	0.76	0.81	**0.83**
12	0.20	**0.39**	0.34	0.08	**0.26**	0.25	**0.56**	0.11	0.23	0.53	0.53	0.53
13	0.24	0.65	0.65	0.12	0.57	0.57	**0.79**	0.74	0.77	0.66	**0.72**	0.69
14	0.27	0.35	**0.39**	0.19	0.04	**0.22**	**0.36**	0.08	0.06	**0.58**	0.29	0.31
15	0.32	0.63	0.63	0.54	0.47	**0.58**	0.73	**0.86**	0.85	0.75	**0.84**	0.83
16	0.13	0.30	0.30	0.21	0.57	**0.58**	**0.92**	0.72	0.83	**0.91**	0.59	0.76
17	0.65	0.68	**0.70**	0.33	0.75	**0.77**	0.93	0.90	**0.94**	0.91	0.93	**0.94**
18	0.89	0.87	**0.90**	0.88	0.87	**0.92**	**0.96**	0.61	0.87	**0.97**	0.63	0.91

Table 5: The Pearson's linear correlation coefficients (PLCC) for DNT and RRED in TID2013 benchmark.

Furthermore, for the luminance distortions, as regards CIELAB, the domination of chrominance is clearly remarked for ten distortion types (1, 2, 3, 4, 5, 6, 7, 8, 15, and 16). Moreover, for the YCbCr, the domination of CI persists with fourteen artifacts (1, 2, 3, 4, 6, 7, 8, 11, 12, 13, 14, 15, 16, and 17). It can be concluded from these results, that for the EMISM method, the CI needs to be invoked for the TID2013 artifacts, especially for luminance distortions.

Regarding WNISM method, the rows representing the chrominance distortions highlighted CI for two cases (1, and 4) for CIELAB, and three cases (1, 2, and 4) for YCbCr. The results of the Chromatic aberrations distortion are already distinctly lower for both color spaces and the deterioration becomes worst with YCbCr. This leads us to conclude that CI is not required in that case, since LI achieved the highest results for this artifact.

Regarding the luminance distortions, the results of CIELAB and YCbCr maintain the advantage of LI for this method, CI has only seven distinctions (1, 2, 3, 4, 5, 15, and 17) for CIELAB and six distinctions (1, 2, 4, 5, 15, and 17) for YCbCr. It appears that the results of this method are widely reflected the crucial requirement of LI for this method.

In the same way, Table IV-A shows the prediction accuracy for both methods DNT and RRED with two color spaces CIELAB and YCbCr.

Let us consider the DNT method. For the chrominance distortions, CI dominates for three cases (1, 2, and 4) for CIELAB and four cases (1, 2, 4, and 5) for YCbCr. While for 3 and 6, LI is required to achieve better results. For the distortion type 5, the YCbCr promoted CI while the CIELAB favored LI.

Concerning luminance distortions, the upper hand goes for CI with twelve artifacts (1, 2, 3, 4, 5, 11, 12, 13, 14, 15, 16, and 17) for CIELAB, and eleven artifacts (1, 2, 3, 4, 5, 6, 11, 12, 13, 16, and 17) for YCbCr. This means that, for the DNT, CI is more relevant than LI. Yet it is on this fact that CI has been attached to this kind of process more than LI.

The second method in Table IV-A is the RRED. This method has provided an equitable process for the selection of CI and LI for YCbCr. Concerning chrominance distortions when the CIELAB components have been awarded, LI outperforms CI for four artifacts (2, 3, 5, and 6). In the other color space, LI shares the same number of cases with CI, moreover, the performances of the distortion type 4 have known an immense deterioration for LI which excludes this latter from this artifact.

Regarding the luminance distortions, almost an equal distribution is reached for the YCbCr color space between LI and CI with nine artifacts for CI and eight artifacts for LI and they share the same PLCC for the distortion type 12, the CIELAB color space grants eight artifacts for CI and ten

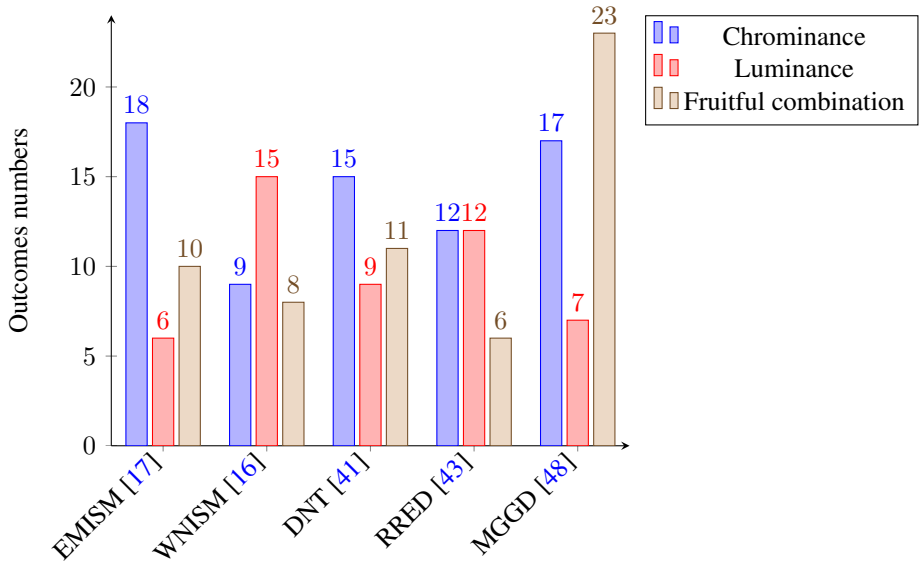

Figure. 6: A holistic view of LI and CI comparison and the fruitful combinations for YCbCr.

for LI. Seeing the quality scores under 0.5, two cases for each color spaces grab our attention. For the CIELAB, the distortion type 12 shows the uselessness of CI for this kind of artifact, nevertheless, whether the usefulness of CI or LI for the distortion type 14 does not exceed the quality score of 0.5.

The aim of this subsection was to examine the impact of CI and LI for different quality assessment methods under study. One thing that makes sense is that CI have to perform quite well for images that have undergone color distortions. Similarly, LI have to perform quite well for images that have undergone luminance distortions. However, experiments show that some cases do not follow this logic. As an example, two color distortions grab our attention: 5 and 6. For these artifacts, results with LI are higher than the ones with CI, this can be noticed for several methods and for both color spaces. However, in such cases, the use of LI or CI independently does not achieve the desired outcome. Therefore, in the next subsection, the combination between LI and CI contributes to the debate in order to find if there a possible improvement can be reached.

B. Combination of luminance and chrominance information

Table III-B.2 shows that the combination does not cause too much improvement to the results of EMISM in terms of artifacts. For chrominance distortions, only two artifacts (5, and 6) for CIELAB and YCbCr have known an amelioration comparing to the results of CI and LI. Regarding luminance distortions, six artifacts (5, 6, 7, 8, 11, and 12) for CIELAB and eight artifacts (5, 6, 7, 8, 11, 12, 15, and 16) for YCbCr have benefited from the combination. Therefore for thirty artifacts, the intended outcome of the combination does not yield as well as the use of LI or CI independently.

Concerning WNISM, when applying the combination to chrominance distortions, a negligible impact has been remarked upon in two artifacts (3, and 4) for both CIELAB and YCbCr. As regards the luminance distortions, Table III-B.2 illustrates a little bit improvement for thirteen cases (seven artifacts (3, 5, 11, 12, 13, 16, and 17) for CIELAB and six artifacts (3, 5, 12, 13, 16, and 17) for YCbCr). Among the twenty-four distortion types in this benchmark, for both color spaces, only the distortion type 14 from the luminance distortions has known a significant improvement with this combination.

The DNT has not known development like that of EMISM and WNISM and has stayed under 0.8 with the combination for chrominance distortions as shown in Table IV-A. The luminance distortions acclaim the combination for five artifacts (10, 11, 14, 17, and 18) for CIELAB. While for YCbCr, six artifacts (10, 11, 14, 15, 17, and 18) have been improved, as for three artifacts (3, 5, and 16), the increase does not exceed $0,01$, which is not a substantial added value.

The combination of CI and LI in Table IV-A for RRED does not seem to be a significant change for chrominance distortions. The same outcome has been remarked for luminance distortions, except for eight cases (four artifacts (5, 6, 11, and 17) for each color space), the combination brings a little bit of improvement.

Figures 6 and 7 show a comparison between LI and CI in terms of the number of distortion types, and illustrate also the number of improvements for each method when considering the combination for YCbCr and CIELAB color spaces, respectively. For the methods EMISM and DNT, CI has performed better than LI in terms of the number of distortion types, unlike the WNISM and the RRED, a clear distinction has been drawn between CI and LI in favor of the second one. Meanwhile, the percentages of fruitful combination did not exceed 50%, meaning that CI or LI alone can produce better results than the combination. Hence, the next subsection aims to give each type of distortion and each method the most appropriate information.

C. Information adaptation

The aim of the information adaptation is to assort each information according to the distortion type. Hence, the correla-

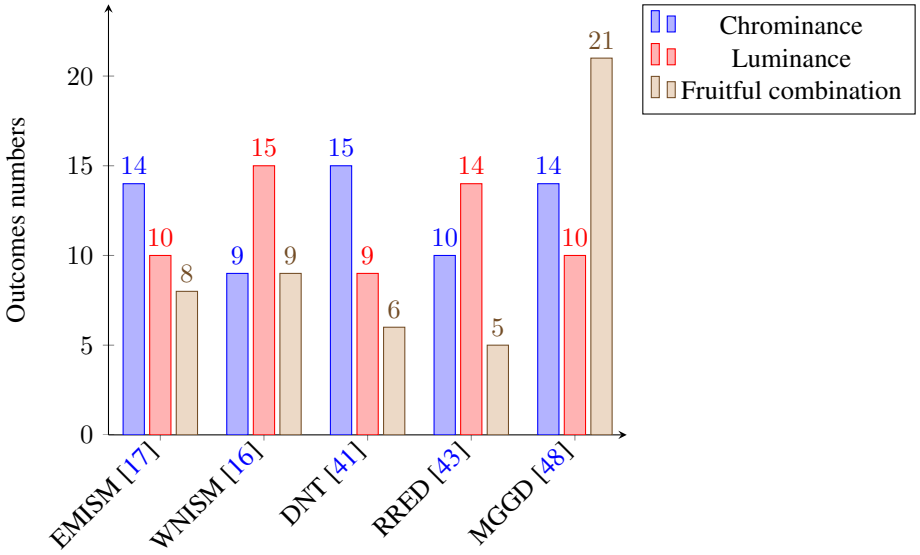

Figure. 7: A holistic view of LI and CI comparison and the fruitful combinations for CIELAB.

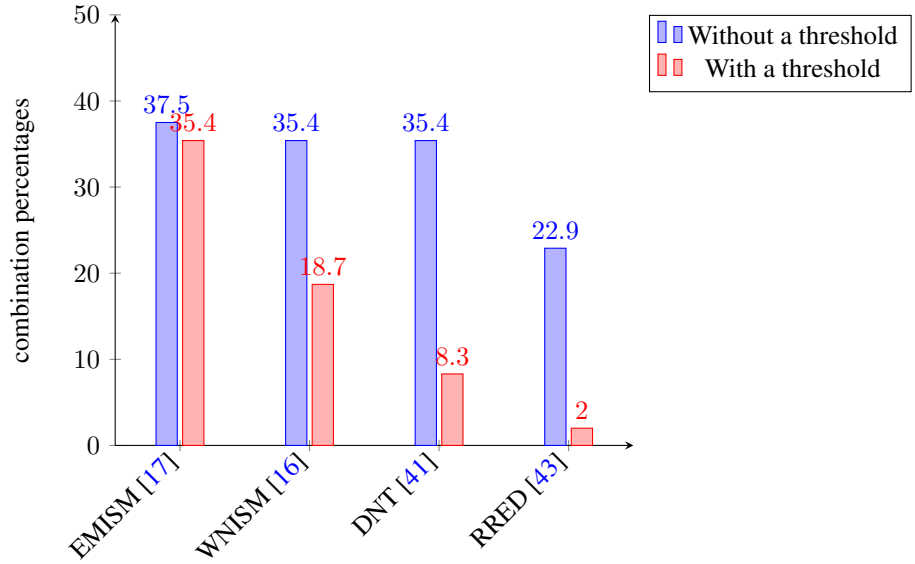

Figure. 8: The percentages of fruitful combination with and without a threshold in TID2013 for both color spaces.

tion between the two selected color spaces to avoid the obstacles affecting the adaptation gives 0.78 between the whole two information which means that both color spaces behave in the same manner, meanwhile, the correlations between each information for each method strengthen the last remark.

Let us take a look at the overall performance of some of well-known correlation coefficients and error measures. Table IV-B presents a comparison between color information impact on the studied methods using Pearson linear correlation coefficient (PLCC), Spearman rank correlation coefficient (SRCC), Kendalls rank correlation coefficient (KRCC), Root mean-squared error (RMSE), and mean absolute error (MAE). The PLCC is computed in order to evaluate the prediction accuracy. SRCC and KRCC are employed to assess prediction monotonicity, they are nonparametric rank order-based correlation metrics. MAE and RMSE are calculated by comparing the subjective and objective scores after nonlinear mapping. A better RRIQA measure should have higher PLCC, SRCC, and KRCC, but lower MAE and RMSE values.

The combination based measures (LCM) dominate almost for all cases, except for two cases. RRED with the luminance component represents the best solution for CIELAB color space, and EMISM with the chrominance information, especially for the color space CIELAB and for the chrominance distortions. These results revealed the effectiveness of the combination when it comes to the entire database.

Table IV-B describes the desired color information adaptation according to section III-B.2. Hence, the categorization is made starting by the types of distortion then for methods. By looking at Table IV-B and regarding the chrominance distortion, the distortion type 1 has needed CI for seven cases against one case for the combination and none for LI. The second chrominance distortion type favored CI for six cases and LI for the remaining two cases. Nonetheless, LI dominates for the distortion type 3 for six cases. Whereas the distortion type 4 proves the meaningless of LI with seven cases

		Chrominance Distortions					Luminance Distortions				
		PLCC	SRCC	KROCC	RMSE	MAE	PLCC	SRCC	KROCC	RMSE	MAE
EMISM	L	0.63	0.62	0.47	11.02	8.38	0.59	0.56	0.41	11.52	9.00
	AB	**0.68**	**0.66**	**0.51**	**10.62**	**7.92**	0.63	0.61	0.46	11.32	8.45
	CIELAB	**0.68**	0.65	**0.51**	10.64	7.94	**0.64**	**0.62**	**0.48**	**11.28**	**8.37**
	Y	0.52	0.51	0.38	11.93	9.31	0.50	0.49	0.33	12.06	9.54
	CbCr	0.60	0.58	0.43	11.52	9.06	0.52	0.51	0.38	11.94	9.32
	YCbCr	**0.63**	**0.62**	**0.48**	**10.98**	**8.35**	**0.60**	**0.58**	**0.43**	**11.41**	**8.89**
WNISM	L	0.66	0.65	0.50	10.82	8.26	**0.74**	0.72	0.53	9.34	7.64
	AB	0.62	0.60	0.47	11.18	8.67	0.65	0.64	0.49	10.84	8.28
	CIELAB	**0.75**	**0.73**	**0.56**	**9.11**	**7.53**	**0.74**	**0.73**	**0.54**	**9.31**	**7.58**
	Y	0.64	0.63	0.48	10.94	8.39	0.70	0.68	0.50	10.12	7.98
	CbCr	0.55	0.52	0.37	11.84	9.31	0.46	0.46	0.30	12.76	10.01
	YCbCr	**0.70**	**0.69**	**0.53**	**10.04**	**7.93**	**0.71**	**0.69**	**0.52**	**9.98**	**7.90**
DNT	L	0.53	0.52	0.37	11.97	9.38	0.52	0.51	0.35	12.05	9.41
	AB	0.57	0.55	0.41	11.78	9.17	0.58	0.57	0.43	11.56	9.17
	CIELAB	**0.65**	**0.64**	**0.49**	**10.84**	**8.28**	**0.63**	**0.62**	**0.47**	**10.99**	**8.36**
	Y	0.42	0.40	0.30	12.91	10.29	0.45	0.44	0.32	12.72	9.99
	CbCr	0.45	0.43	0.32	12.75	10.02	0.54	0.54	0.39	11.83	9.24
	YCbCr	**0.56**	**0.54**	**0.41**	**11.77**	**9.17**	**0.62**	**0.61**	**0.43**	**11.22**	**8.68**
RRED	L	**0.82**	**0.81**	**0.60**	**8.18**	**6.53**	**0.78**	**0.76**	**0.55**	**8.87**	**7.03**
	AB	0.75	0.74	0.53	9.02	7.25	0.70	0.69	0.50	9.27	7.57
	CIELAB	0.80	0.79	0.59	8.56	6.77	0.76	0.75	0.54	8.91	7.04
	Y	0.71	0.69	0.50	9.13	7.42	0.81	0.79	0.60	8.23	6.64
	CbCr	0.74	0.73	0.54	8.79	7.01	0.75	0.73	0.55	8.71	6.87
	YCbCr	**0.80**	**0.79**	**0.58**	**8.33**	**6.64**	**0.80**	**0.79**	**0.59**	**8.37**	**6.70**
MGGD	L	0.56	0.54	0.40	11.77	9.17	0.57	0.55	0.40	11.71	9.11
	AB	0.59	0.58	0.42	11.58	9.00	0.58	0.56	0.41	11.61	8.98
	CIELAB	**0.90**	**0.87**	**0.68**	**6.96**	**5.23**	**0.85**	**0.84**	**0.63**	**7.23**	**5.65**
	Y	0.39	0.37	0.20	13.15	10.43	0.51	0.49	0.37	11.98	9.41
	CbCr	0.54	0.52	0.38	11.71	9.27	0.57	0.56	0.41	11.78	9.15
	YCbCr	**0.89**	**0.86**	**0.63**	**7.03**	**5.36**	**0.85**	**0.83**	**0.62**	**7.31**	**5.67**

Table 6: A comparison between the four selected methods using three correlation coefficients and two error measures.

for CI and one case for the combination. The remaining two chrominance distortions do not benefit from CI over LI and combination, starting with 5, only one case has stood for CI against five and two for LI and combination respectively. CI has been neglected for 6 with six cases for LI and two for combination. The results of the chrominance distortions deducted that the CI has dominated for twenty three cases against nineteen cases for LI and only six cases for the combination, which sustain the CI.

Let us turn to luminance distortions, CI dominates for five artifacts (1, 2, 3, 4, and 15) with a score of eight (two color spaces for four methods) for the first two artifacts and the High frequency noise, which means that CI can be the only information used for these kinds of degradations, furthermore, the Multiplicative Gaussian noise gives seven cases for CI and one for LI, proving the effectiveness of CI for this distortion type.

LI attends for eight distortion types (6, 7, 8, 9, 10, 14, 16, and 18) as the most efficient information. Thus, the use of CI alone is not sufficient for these artifacts. Indeed, CI has been appeared only once in JPEG2000 transmission errors and three times in comfort noise. These results depicted the effectiveness of LI for these kinds of degradations, regarding these artifacts, they are based on data transmission, while neglecting CI.

Finally, the combination between both information is best suited only for two distortions (5, and 11).

To sum up, the proposed protocol using a threshold obviously offers a better adaptation than in normal cases. Without a threshold, the combination has 63 cases, which increases the features size. However, with a threshold, the combination has only 31 cases, which gives more accuracy in terms of features size and correlation with MOS. Figure 8 proves without a doubt that the use of a threshold reduces the size of features for the four selected methods. Looking at the percentages, the combination has been needed only for 2% for RRED when the threshold is considered.

V. Conclusion

According to the results of this paper, the chrominance channels are indispensable for RRIQA methods and for both color spaces under study. Nonetheless, the combination does not look to be appropriate for the four selected methods. The human eye perceives the diffusion as a mixture of the colors within it. Thus, the artifacts do not only alter the components

Label	EMISM		WNISM		DNT		RRED	
	CIELAB	YCbCr	CIELAB	YCbCr	CIELAB	YCbCr	CIELAB	YCbCr
	Chrominance distortions							
1	AB	CbCr	AB	CbCr	AB	CbCr	AB	YCbCr
2	AB	CbCr	L	CbCr	AB	CbCr	L	CbCr
3	AB	CbCr	L	Y	L	Y	L	Y
4	AB	CbCr	AB	YCbCr	AB	CbCr	AB	CbCr
5	CIELAB	YCbCr	L	Y	L	CbCr	L	Y
6	CIELAB	YCbCr	L	Y	L	Y	L	Y
	Luminance distortions							
1	AB	CbCr	AB	CbCr	AB	CbCr	AB	CbCr
2	AB	CbCr	AB	CbCr	AB	CbCr	AB	CbCr
3	AB	CbCr	CIELAB	YCbCr	AB	CbCr	AB	Y
4	AB	CbCr	AB	CbCr	AB	CbCr	AB	CbCr
5	CIELAB	YCbCr	CIELAB	YCbCr	L	CbCr	AB	CbCr
6	CIELAB	YCbCr	L	Y	L	Y	L	Y
7	CIELAB	YCbCr	L	Y	L	Y	L	Y
8	CIELAB	YCbCr	L	Y	L	Y	L	Y
9	L	Y	L	Y	L	Y	L	Y
10	L	Y	L	Y	CIELAB	Y	L	CbCr
11	CIELAB	YCbCr	CIELAB	Y	CIELAB	YCbCr	L	CbCr
12	CIELAB	YCbCr	CIELAB	Y	AB	CbCr	L	Y
13	L	CbCr	L	Y	AB	CbCr	L	CbCr
14	L	Y	L	Y	CIELAB	Y	L	Y
15	AB	CbCr	AB	CbCr	AB	Y	AB	CbCr
16	AB	YCbCr	L	Y	AB	CbCr	L	Y
17	L	CbCr	CIELAB	YCbCr	AB	CbCr	L	Y
18	L	Y	L	Y	L	Y	L	Y

Table 7: The categorization of the three information according to the adaptation protocol in subsection III-B.2.

but also the dependencies between them. Thus, the comparison has been enhanced by a compatible RRIQA based color method which uses multivariate generalized Gaussian distribution MGGD [48] to capture dependencies between color components.

For Table IV-B, the combination has significantly improved the scores, for the MGGD, with more than 0.2 improvement. Figures 6 and 7 strengthen the effectiveness of this kind of process with 44 cases of improvement from 48 (23 for YCbCr, and 21 for CIELAB).

Moreover, the proposed protocol of adaptation leads to a better coherence and adequacy of the correlation coefficients. Table IV-B shows the categorization of the three information (LI, CI, Combination) using the adaptation protocol, LI is more suited to eleven types of distortion, followed by CI which is appropriate to eight distortion types, whereas the combination of both of them, is favored for application only in two distortion types.

As a future work, we plan to develop these four aforementioned methods while benefiting from the color information and the dependencies between color components according to MGGD results. Furthermore, We are interested in enhancing the proposed protocol of adaption and in studying other color spaces.

Acknowledgments

This work has been supported by the project CNRS-CNRST STIC 02/2014.

References

[1] L. Li, Y. Yan, Z. Lu, J. Wu, K. Gu, and S. Wang, "No-reference quality assessment of deblurred images based on natural scene statistics," *IEEE Access*, vol. 5, pp. 2163–2171, 2017.

[2] D. Lee and K. N. Plataniotis, "Towards a full-reference quality assessment for color images using directional statistics," *IEEE Transactions on Image Processing*, vol. 24, pp. 3950–3965, Nov 2015.

[3] Q. Li, W. Lin, and Y. Fang, "No-reference quality assessment for multiply-distorted images in gradient domain," *IEEE Signal Processing Letters*, vol. 23, pp. 541–545, April 2016.

[4] H. R. Sheikh, M. F. Sabir, and A. C. Bovik, "A statistical evaluation of recent full reference image quality assessment algorithms," *IEEE Transactions on Image Processing*, vol. 15, pp. 3440–3451, Nov 2006.

[5] H. R. Wu and M. Yuen, "A generalized block-edge impairment metric for video coding," *IEEE Signal Processing Letters*, vol. 4, pp. 317–320, Nov 1997.

[6] Z. Wang, A. C. Bovik, and B. L. Evan, "Blind measurement of blocking artifacts in images," in *Image Processing, 2000. Proceedings. 2000 International Conference on*, vol. 3, pp. 981–984 vol.3, 2000.

[7] Z. Yu, H. R. Wu, S. Winkler, and T. Chen, "Vision-model-based impairment metric to evaluate blocking artifacts in digital video," *Proceedings of the IEEE*, vol. 90, pp. 154–169, Jan 2002.

[8] Z. Wang, H. R. Sheikh, and A. C. Bovik, "No-reference perceptual quality assessment of jpeg compressed images," in *Image Processing. 2002. Proceedings. 2002 International Conference on*, vol. 1, pp. I–477–I–480 vol.1, 2002.

[9] X. Li, "Blind image quality assessment," in *Image Processing. 2002. Proceedings. 2002 International Conference on*, vol. 1, pp. I–449–I–452 vol.1, 2002.

[10] H. R. Sheikh, A. C. Bovik, and L. Cormack, "No-reference quality assessment using natural scene statistics: Jpeg2000," *IEEE Transactions on Image Processing*, vol. 14, pp. 1918–1927, Nov 2005.

[11] P. Marziliano, F. Dufaux, S. Winkler, and T. Ebrahimi, "Perceptual blur and ringing metrics: Application to jpeg2000, signal process," *Image Commun*, pp. 163–172, 2004.

[12] M. Gunawan, I.P.;Ghanbari, "Reduced-reference picture quality estimation by using local harmonic amplitude information," in *Proc. London Communications Symposium 2003, University College London, UK, 8-9 September 2003*, pp. 137–140, N/A, 2003.

[13] T. M. Kusuma and H. J. Zepernick, "A reduced-reference perceptual quality metric for in-service image quality assessment," in *Mobile Future and Symposium on Trends in Communications, 2003. SympoTIC '03. Joint First Workshop on*, pp. 71–74, Oct 2003.

[14] R. R. Pastrana-Vidal, J. C. Gicquel, C. Colomes, and H. Cherifi, "Sporadic frame dropping impact on quality perception," vol. 5292, pp. 182–193, 2004.

[15] M. Carnec, P. Le Callet, and D. Barba, "Visual features for image quality assessment with reduced reference," in *Image Processing, 2005. ICIP 2005. IEEE International Conference on*, vol. 1, pp. I–421–4, Sept 2005.

[16] Z. Wang and E. P. Simoncelli, "Reduced-reference image quality assessment using a wavelet-domain natural image statistic model," in *Proc. SPIE, Conf. on Human Vision and Electronic Imaging, X* (B. Rogowitz, T. N. Pappas, and S. J. Daly, eds.), vol. 5666, (San Jose, CA), pp. 149–159, Jan 17-20 2005.

[17] A. A. Abdelouahad, M. E. Hassouni, H. Cherifi, and D. Aboutajdine, "Reduced reference image quality assessment based on statistics in empirical mode decomposition domain," *Signal, Image and Video Processing*, vol. 8, no. 8, pp. 1663–1680, 2014.

[18] Y. Niu, H. Zhang, W. Guo, and R. Ji, "Image quality assessment for color correction based on color contrast similarity and color value difference," *IEEE Transactions on Circuits and Systems for Video Technology*, vol. PP, no. 99, pp. 1–1, 2017.

[19] L. Li, W. Xia, Y. Fang, K. Gu, J. Wu, W. Lin, and J. Qian, "Color image quality assessment based on sparse representation and reconstruction residual," *Journal of Visual Communication and Image Representation*, vol. 38, no. Supplement C, pp. 550 – 560, 2016.

[20] W. Zhou, G. Jiang, M. Yu, F. Shao, and Z. Peng, "Reduced-reference stereoscopic image quality assessment based on view and disparity zero-watermarks," *Signal Processing: Image Communication*, vol. 29, no. 1, pp. 167 – 176, 2014.

[21] S. Decherchi, P. Gastaldo, R. Zunino, E. Cambria, and J. Redi, "Circular-elm for the reduced-reference assessment of perceived image quality.," *Neurocomputing*, vol. 102, pp. 78–89, 2013.

[22] J. Redi, P. Gastaldo, I. Heynderickx, and R. Zunino, "Color distribution information for the reduced-reference assessment of perceived image quality.," *IEEE Trans. Circuits Syst. Video Techn.*, vol. 20, no. 12, pp. 1757–1769, 2010.

[23] L. He, D. Wang, X. Li, D. Tao, X. Gao, and F. Gao, "Color fractal structure model for reduced-reference colorful image quality assessment," in *Neural Information Processing - 19th International Conference, ICONIP 2012, Doha, Qatar, November 12-15, 2012, Proceedings, Part II*, pp. 401–408, 2012.

[24] M. Omari, M. E. Hassouni, H. Cherifi, and A. A. Abdelouahad, "On color image quality assessment using natural image statistics," in *Tenth International Conference on Signal-Image Technology and Internet-Based Systems, SITIS 2014, Marrakech, Morocco, November 23-27, 2014*, pp. 516–523, 2014.

[25] D. Ghadiyaram and A. C. Bovik, "Scene statistics of authentically distorted images in perceptually relevant color spaces for blind image quality assessment," in *Image Processing (ICIP), 2015 IEEE International Conference on*, pp. 3851–3855, Sept 2015.

[26] Z. Wan, F. Qi, Y. Liu, and D. Zhao, "Reduced reference stereoscopic image quality assessment based on entropy of classified primitives," in *2017 IEEE International Conference on Multimedia and Expo (ICME)*, pp. 73–78, July 2017.

[27] M. Liu, K. Gu, G. Zhai, P. L. Callet, and W. Zhang, "Perceptual reduced-reference visual quality assessment for contrast alteration," *IEEE Transactions on Broadcasting*, vol. 63, pp. 71–81, March 2017.

[28] S. Golestaneh and L. J. Karam, "Reduced-reference quality assessment based on the entropy of dwt coefficients of locally weighted gradient magnitudes," *IEEE Transactions on Image Processing*, vol. 25, pp. 5293–5303, Nov 2016.

[29] S. A. Golestaneh and L. J. Karam, "Reduced-reference synthesized-texture quality assessment based on multi-scale spatial and statistical texture attributes," in *2016 IEEE International Conference on Image Processing (ICIP)*, pp. 3783–3786, Sept 2016.

[30] A. Chetouani, "A reduced reference image quality assessment for multiply distorted images," in *2015 IEEE/ACS 12th International Conference of Computer Systems and Applications (AICCSA)*, pp. 1–4, Nov 2015.

[31] A. Balanov, A. Schwartz, and Y. Moshe, "Reduced-reference image quality assessment based on dct subband similarity," in *2016 Eighth International Confer-*

ence on Quality of Multimedia Experience (QoMEX), pp. 1–6, June 2016.

[32] I. C. on Illumination, *Colorimetry*. CIE technical report, Commission internationale de l'Eclairage, CIE Central Bureau, 2004.

[33] L. He, X. Gao, W. Lu, X. Li, and D. Tao, "Image quality assessment based on s-cielab model," *Signal, Image and Video Processing*, vol. 5, no. 3, pp. 283–290, 2011.

[34] M. Hassan and C. Bhagvati, "Article: Structural similarity measure for color images," *International Journal of Computer Applications*, vol. 43, pp. 7–12, April 2012. Full text available.

[35] U. Rajashekar, Z. Wang, and E. P. Simoncelli, "Perceptual quality assessment of color images using adaptive signal representation," in *Proc SPIE, Conf. on Human Vision and Electronic Imaging, XV* (B. Rogowitz and T. N. Pappas, eds.), vol. 7527, (San Jose, CA), Optical Society of America, Jan 18-21 2010.

[36] V. Vezhnevets, V. Sazonov, and A. Andreeva, "A survey on pixel-based skin color detection techniques," in *IN PROC. GRAPHICON-2003*, pp. 85–92, 2003.

[37] J. Yang, W. Lu, and A. Waibel, "Skin-color modeling and adaptation," pp. 687–694, 1997.

[38] P. Kakumanu, S. Makrogiannis, and N. Bourbakis, "A survey of skin-color modeling and detection methods," *Pattern Recognition*, vol. 40, no. 3, pp. 1106 – 1122, 2007.

[39] F. N. I. and S. P., "Graphical assessment of dependence: Is a picture worth 100 tests?," *The American Statistician*, vol. 55, pp. 233–239, 2001.

[40] E. Simoncelli and W. Freeman, "The steerable pyramid: a flexible architecture for multi-scale derivative computation," in *Image Processing, 1995. Proceedings., International Conference on*, vol. 3, pp. 444–447 vol.3, Oct 1995.

[41] Q. Li and Z. Wang, "Reduced-reference image quality assessment using divisive normalization-based image representation," *Selected Topics in Signal Processing, IEEE Journal of*, vol. 3, pp. 202–211, April 2009.

[42] M. J. Wainwright and E. P. Simoncelli, "Scale mixtures of Gaussians and the statistics of natural images," in *Adv. Neural Information Processing Systems (NIPS*99)* (S. A. Solla, T. K. Leen, and K.-R. Müller, eds.), vol. 12, (Cambridge, MA), pp. 855–861, MIT Press, May 2000.

[43] R. Soundararajan and A. Bovik, "Rred indices: Reduced reference entropic differencing for image quality assessment," *Image Processing, IEEE Transactions on*, vol. 21, pp. 517–526, Feb 2012.

[44] N. Ponomarenko, L. Jin, O. Ieremeiev, V. Lukin, K. Egiazarian, J. Astola, B. Vozel, K. Chehdi, M. Carli, F. Battisti, and C.-C. J. Kuo, "Image database tid2013: Peculiarities, results and perspectives," *Signal Processing: Image Communication*, vol. 30, pp. 57 – 77, 2015.

[45] N. Ponomarenko, O. Ieremeiev, V. Lukin, K. Egiazarian, L. Jin, J. Astola, B. Vozel, K. Chehdi, M. Carli, F. Battisti, and C.-C. Kuo, "Color image database tid2013: Peculiarities and preliminary results," in *Visual Information Processing (EUVIP), 2013 4th European Workshop on*, pp. 106–111, June 2013.

[46] N. N. Ponomarenko, V. V. Lukin, A. A. Zelensky, K. Egiazarian, M. Carli, and F. Battisti, "Tid2008: a database for evaluation of full-reference visual quality assessment metrics," *Adv. Modern Radioelectron*, p. 3045, 10 2009.

[47] http://www.vqeg.org, "Vqeg rrnr-tv group test plan," vol. Draft version 1.7, pp. 2004.6.21[E-B/OL],2005.1.10.

[48] M. Omari, M. E. Hassouni, A. A. Abdelouahad, and H. Cherifi, "A statistical reduced-reference method for color image quality assessment," *Multimedia Tools and Applications*, vol. 74, no. 19, pp. 8685–8701, 2015.

Author Biographies

Mounir Omari is a PhD candidate at the University of Mohammed V-Agdal. His research deals with the color in the quality assessment.

Abdelkaher Ait Abdelouahad received the PhD from the University of Mohammed V-Agdal in 2013. Currently, he is an assistant professor at University of Agadir. His research focuses on the image quality assessment area.

Mohammed El Hassouni received the PhD in image and video processing from the University of Burgundy in 2005. He joined University Mohammed V-Agdal- as assistant professor since 2006 and associate professor since 2012. He was a visitor of several universities (Bordeaux I, Orlans, Dijon and Konstanz). He is member of IEEE and IEEE Signal Processing Society. His research focuses on image analysis, quality assessment and mesh processing. His application areas are medical imaging, biometry and QoE.

Hocine Cherifi has been Professor of Computer Science at the University of Burgundy, France, since 1999. Prior to moving to Dijon, he held faculty positions at Rouen University and Jean Monnet University, in the disciplines of Signal Processing and Mathematics. He has held visiting positions at Yonsei, Korea, University of Western Australia, Australia, National Pintung University, Taiwan, and Galatasaray University, Turkey.He has been an Associate Editor of a variety of image processing and computer vision journals. More recently, he joined the editorial board of the Computational Social Networks Journal published by Springer. He received a PhD in Signal Processing from the Grenoble Institute of Technology, France in 1984. His research focuses on the fields of computer vision and complex networks.